### CONFERENCE PRE-PRINT

# NONINDUCTIVE STARTUP OF SPHERICAL TOKAMAK WITH REDUCED TRAPPED ELECTRONS BY ELECTRON BERNSTEIN WAVE HEATING AND CURRENT DRIVE ON LATE

M. UCHIDA, H. TANAKA, H. ETOU, T. TAIGA, H. SHINOHARA, A. NAKAI, R. HIRAYAMA Graduate School of Energy Science, Kyoto University Kyoto, Japan

Email: m-uchida@energy.kyoto-u.ac.jp

#### **Abstract**

Start up and formation of an overdense spherical tokamak by electron Bernstein waves with the microwave injection from bottom port in order to suppress trapped electrons has been investigated in the Low Aspect ratio Torus Experiment (LATE) device. The experimental results show that the development of trapped electrons outside the last closed flux surface are suppressed compared with the midplane outboard injection case, suggesting the improved coupling to current carrying passing electrons. The results also suggest that the bottom injection is advantageous for heating at the plasma core without the second harmonic heating in the peripheral region.

### 1. INTRODUCTION

There has been considerable interest in the noninductive start-up of Tokamak without the use of the central solenoid (CS). If the plasma current can be started up noninductively, the CS can be reduced or even eliminated from the Tokamak device, which brings about significant technical advantage. For Spherical Tokamak (ST) based fusion devices, elimination of CS is crucial since there is only a limited space in the centre column to maintain a small aspect ratio. Electron cyclotron heating and current drive (ECH/ECCD) is an attractive tool for the noninductive startup since electron cyclotron (EC) waves can be injected through a small launcher remote from the plasma.

In the LATE device it was shown that electron Bernstein (EB) waves can rapidly ramp up the plasma current as fast as  $\sim 260$  kA/s, comparable to the lower hybrid ramp-up rate [1], and also can start up and form an extremely overdense tokamak plasma in which the electron density reaches as high as 7 times the plasma cutoff density [2-4]. In these previous experiments, however, trapped electrons were significantly developed in energy and density outside the last closed flux surface (LCFS) and they were lost to the vacuum vessel wall via pitch angle scatterings. Heat flow to the limiters at top, bottom and outboard side of the vacuum vessel show that the total loss power to the limiters accounts for  $\sim 70$  percent of the injected power, resulting in a severe degradation in current drive efficiency.

For the microwave injection from the outboard midplane launcher, EC or EB waves are initially absorbed by trapped electrons located outside the LCFS, followed by absorption by passing electrons. To suppress trapped electrons outside the LCFS, a new bottom port launcher has been installed on the LATE device. In this configuration, the absorption by trapped electrons outside the LCFS is expected to be reduced since the waves do not pass through the midplane outboard region where the density of trapped electrons is high. In the paper, we report on an experiment of ST startup by EC waves launched from the bottom port, in which the development of trapped electrons is significantly suppressed compared to the case of microwave injection from the midplane outboard port.

### 2. EXPERIMENTAL SETUP

Experiments are conducted on LATE [5]. The vacuum vessel is a stainless-steel cylinder with an inner diameter of 1 m and a height of 1m, as shown Figure 1. The device does not have a central solenoid for inductive current

drive, and the centre post contains only the toroidal magnetic field coils. Therefore, plasma current is initiated and ramped up solely by microwaves power. There are four 2.45 GHz,  $\sim$ 20 kW, 2 s magnetrons, and two of them were used for the experiment. The maximum toroidal field is 0.16 T at the centre of the device (R = 0.25 m). There are three pairs of vertical field coils whose currents are provided by independent power supplies. The time evolution of the strength and field index of the vertical field  $B_v$  is controlled by adjusting the current in each coil according to a pre-programmed sequence.

A new bottom port launcher has been installed on the LATE device as shown in Figure 1. The angle of launcher is 15 degrees from the vertical and its central axis intersects the midplane at R=0.18 m. The power is injected through an open circular waveguide antenna with an inner diameter of 134 mm. The injection mode is O-mode for the mode-conversion to EB waves via O-X-B method. After the mode conversion the parallel refractive index  $N_{\parallel}$  of EB waves upshifts as the waves propagate inward when the waves are below the midplane for the present magnetic configuration of LATE. Ray tracing results of EB waves started from the upper hybrid resonance (UHR) below the midplane show that  $N_{\parallel}$  typically upshifts to more than one due to the poloidal component of magnetic field even if  $N_{\parallel}$  is initially  $\sim 0$  at the UHR.

There are three midplane outboard launchers for 2.45 GHz microwaves. The power is lauched obliquely to the toroidal field via a cylindrical laucher of open waveguide type in the form of O-mode.

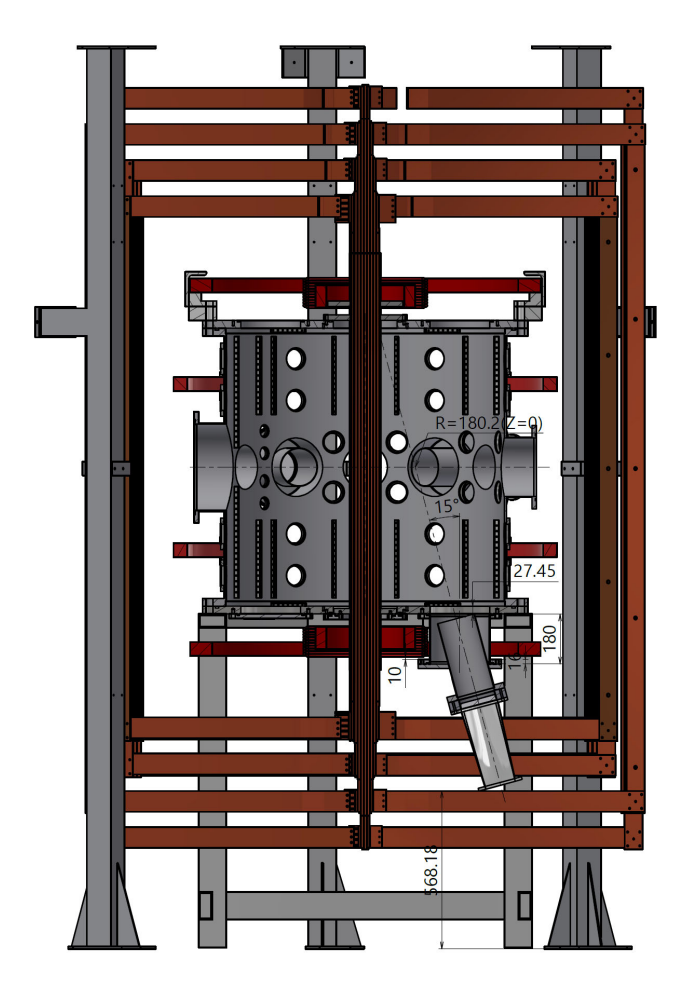


FIG. 1. LATE device and with the bottom launcher for 2.45GHz microwave.

### 3. EXPERIMENTAL RESULTS AND DISCUSSION

Figure 2 shows the typical discharges comparing the bottom (red) and the midplane outboard (black) injection. When a microwave power of  $P_{\rm inj} \sim 8\,$  kW is injected under a weak  $B_v$  field of  $\sim 15\,$  G, a plasma is initiated at

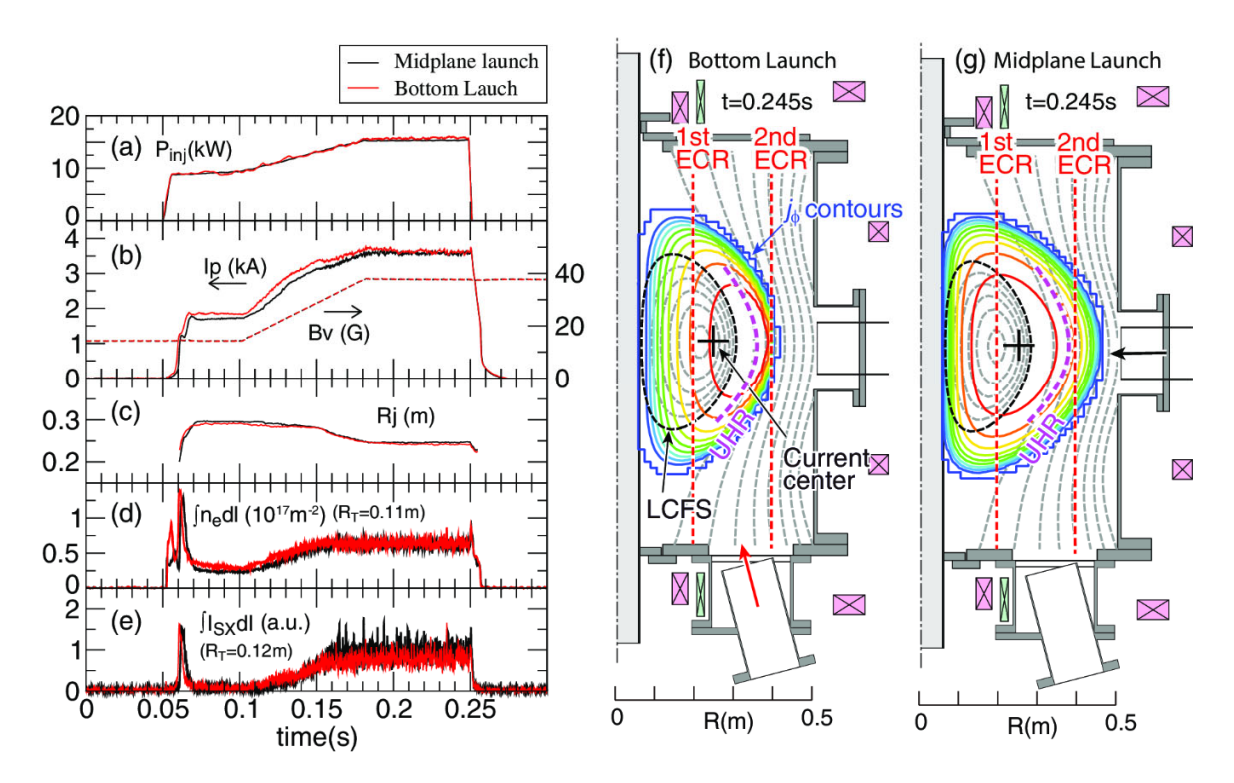


FIG. 2. Typical discharges for bottom (red) and midplane (black) injection. Time traces of (a) injected microwave power, (b) plasma current and  $B_v$ , (c) radial position of plasma current centre, (d) line-integrated density along a tangent radius of  $R_t = 0.11m$  on midplane, (e) soft X-ray intensity along  $R_t = 0.12m$  on midplane. (f), (g)Current density (colour) and poloidal flux contours (grey). Contours are equally spaced. The 1st and 2nd ECR layer are shown in red dash lines.

the fundamental EC resonance layer. After a while, a plasma current is initiated and quickly increases up to  $\sim$  2 kA, resulting in a formation of closed flux surfaces (t=0.07 s) under the steady vertical field [6]. Then, the plasma current ramps up with ramps of the microwave power and  $B_v$ , and finally reaches  $I_p \sim 3.6$  kA, after which the plasma is maintained steady until the end of microwave pulse. The soft X-ray signal appears and increases with  $I_p$  as shown in Fig. 2(e), suggesting the current is carried by EB-wave driven fast electron tail [1].

The plasma current of bottom injection is slightly higher than that of midplane injection throughout the discharge (Fig.2 (b)), suggesting an improved efficiency in current generation, although the difference in  $I_p$  is not large since the equilibrium vertical field strength  $B_v$ , which is pre-programmed, constrains  $I_p$ . The traces of radial position of plasma current centre, line-integrated density, and soft X-ray intensity (Figs. 2(c), (d), and (e)) are almost the same for both cases. Figures 2(f) and 2(g) show current density and poloidal flux contours at t=0.245 s estimated by the magnetic analysis [1] for bottom and midplane injection, respectively. The current distribution for midplane injection is significantly extended to the lower field side, indicating the development of trapped electrons outside the LCFS. On the other hand, they are suppressed for the bottom injection case.

The equilibrium pressure profiles are obtained using the equation for anisotropic pressure,  $\mathbf{j} \times \mathbf{B} = \nabla \cdot \mathbf{P}$ , where  $\mathbf{P} = p_{\perp}\mathbf{I} + (p_{\parallel} - p_{\perp}) \mathbf{B} \mathbf{B}/B^2$  and  $\nabla \cdot \mathbf{j} = 0$ , where  $p_{\parallel} = n_e m \langle \gamma v_{\parallel} v_{\parallel} \rangle_v$  and  $p_{\perp} = n_e m \langle \gamma v_{\perp} v_{\perp} \rangle_v$  are parallel and perpendicular pressure,  $\gamma$  is the relativistic factor,  $\parallel$  and  $\perp$  denote the parallel and perpendicular components to the magnetic field respectively, and  $\langle \cdot \rangle_v$  the average over the velocity space [1]. Figures 3(a) and (b) show sum pressure distributions of  $p_{\parallel} + p_{\perp}$ . Radial profiles of  $p_{\parallel}$  and  $p_{\perp}$  on midplane are shown in Figs. 3(c) and (d). These indicates that the large  $p_{\perp}$  region outside the LCFS is suppressed (Fig. 3(d)) and, on the other hand,  $p_{\parallel}$  near the magnetic axis increased (Fig.3(c)) in the case of bottom injection. Volume integrals of  $p_{\perp}$  and  $p_{\parallel}$  in the bottom injection case are 10 % lower and 20 % higher than those in the midplane injection, respectively. These indicates that trapped electrons outside LCFS are suppressed and efficient development of current carrying passing electrons are realized.

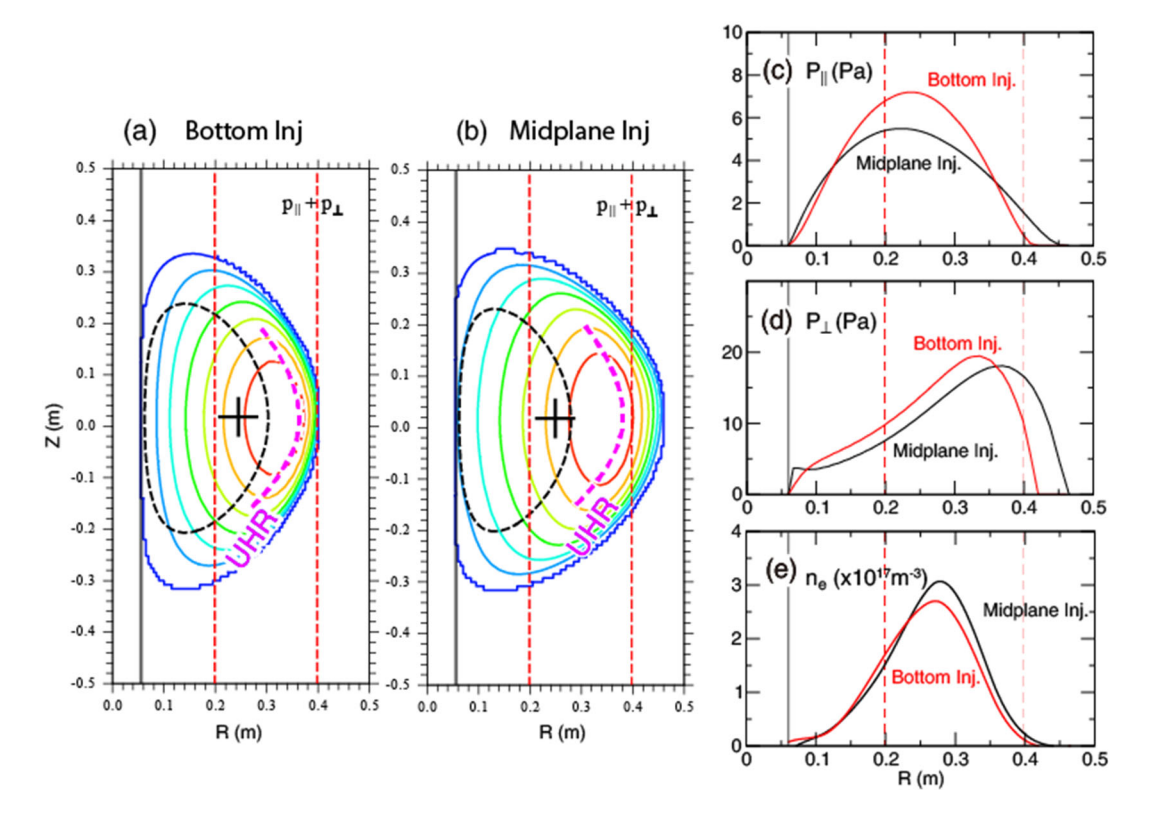


FIG. 3. Profiles of various quantities of the plasma at t=0.245 s in Fig. 2. (a) and (b)  $p_{\parallel}+p_{\perp}$  for Bottom and Midplane injection. (c) and (d) radial profiles of  $p_{\parallel}$  and  $p_{\perp}$  on midplane. (e) ne profile on midplane obtained with Avel inversion technique based on 4-chord measurement of line-integrated density on midplane.

The electron density profiles are estimated with the 4-chord measurement of line-integrated density at tangent radii of  $R_T = 0.11, 0.19,$ 0.27, 0.355 m on midplane, where the local density profiles are obtained with Abel inversion method for interpolated profiles of line-integrated density with the natural cubic spline function. The upper hybrid resonances are estimated to lie on the higher filed side of the 2nd ECR layer for both cases as shown in Figs. 3(a) and (b). Then EB waves mode converted from the incident electromagnetic waves propagate in their first propagation band (between the fundamental and 2nd ECR layer) toward the fundamental ECR layer may heat the bulk electrons as well as the fast electrons [2] for both cases. Trapped electrons extended outside the 2nd ECR layer for the midplane injection (Fig. 3(b)) may be attributed to the 2nd ECR heating by the incident electromagnetic waves. On the other hand, the development of such trapped electrons is suppressed for the bottom injection case, as the heating at the 2nd ECR layer is reduced.

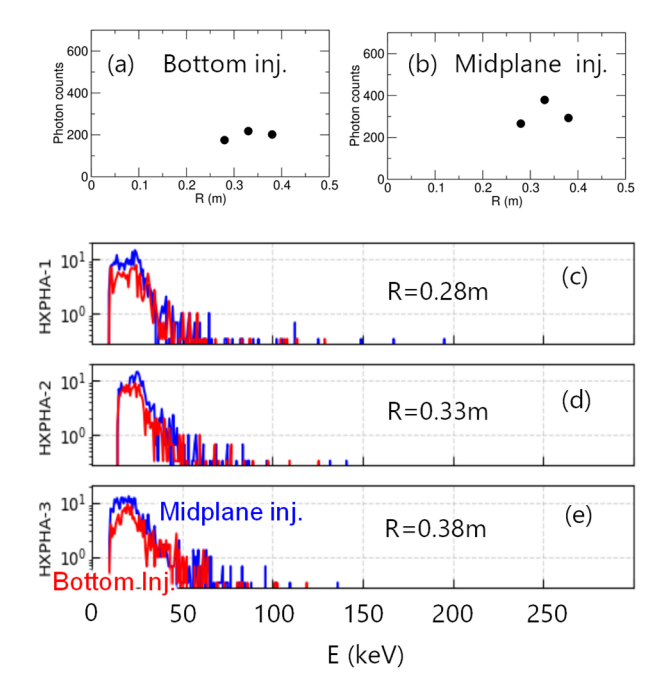


FIG. 4. (a), (b) Photon counts in 25 - 100 keV for bottom and midplane injection measured along three vertical chords, (c)-(e) X-ray spectra along vertical chords of R = 0.28, 0.33, and 0.38 m.

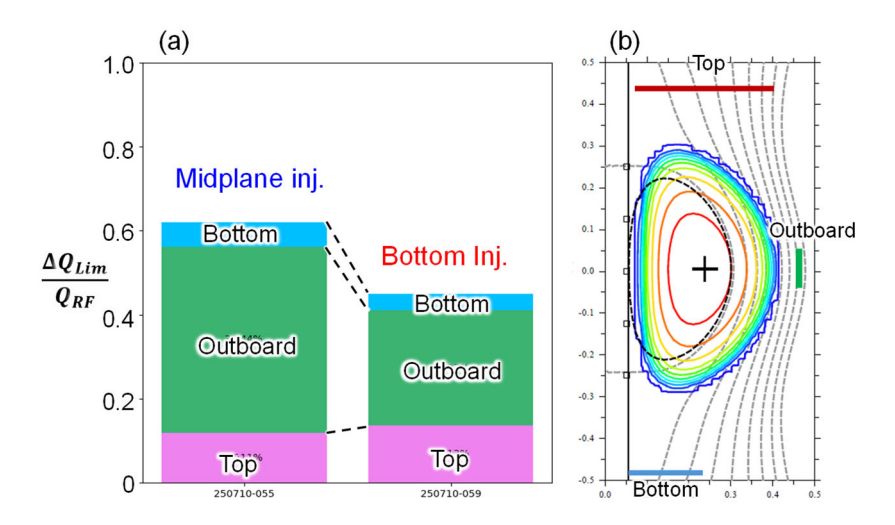


FIG. 5. (a) Heat flow to bottom, outboard and top limiters relative to injected microwave energy in one shot for midplane and bottom injection case, (b) locations of limiters.

Figure 4 shows hard X-ray spectra obtained along three vertical chords at R = 0.28, 0.33, and 0.38 m, most of which are located outside the LCFS. Although the energy range of the X-ray spectra does not change much in both cases (Figs. 4 (c), (d), and (e)), photon counts for the bottom injection are significantly decreased in all chords compared to the case of midplane injection as shown in Figs. 4(a) and (b). These suggest that the number of trapped electrons are reduced outside the LCFS for the bottom injection case.

Trapped electrons will be lost to radial, bottom, or top limiter via pitch angle scatterings. Figure 5(a) shows heat flow to the limiters located at top, outboard, and bottom of the vacuum vessel as shown in Fig.5 (b). The total losses to the radial, bottom and top estimated from the temperature rise of the limiters for the midplane and bottom injection account for  $\sim 62$ % and  $\sim 45$ % of the injected microwave energy in one shot, respectively, indicating the spatial loss to the limiters is reduced by  $\sim 27$ % for the bottom injection. These observations indicate that the microwave absorption by trapped electrons is suppressed and efficient coupling to EB waves in the first propagation band is realized in the bottom injection case.

In summary, start up and formation of an overdense spherical tokamak by electron Bernstein waves with the microwave injection from bottom port to suppress trapped electrons has been investigated in the LATE device. The comparison between the midplane and bottom injection cases shows that the development of trapped electrons outside the last closed flux surface is suppressed for the bottom injection case, suggesting improved coupling to current carrying passing electrons. The results also suggest that the bottom injection is advantageous for heating at the plasma core without the second harmonic heating in the peripheral region.

### **ACKNOWLEDGEMENTS**

This work was supported by JSPS KAKENHI Grant Number JP24K00610.

## REFERENCES

[1] UCHIDA, M., YOSHINAGA, T., TANAKA, T., MAEKAWA, T., "Rapid current ramp-up by cyclotron-driving electrons beyond runaway velocity", Phys. Rev. Lett. **104** 065001 (2010).

#### IAEA-CN-316/2832

- [2] UCHIDA, M. et al., "Noninductive formation of spherical tokamak at 7 times the plasma cutoff density by electron Bernstein wave heating and current drive on LATE", Proc. 24th IAEA Fusion Energy Conference, San Diego, U.S.A. 2012, IAEA-CN-197, EX/P6-18.
- [3] TANAKA, H. et al., "Non-inductive production of extremely overdense spherical tokamak plasma by electron Bernstein wave excited via O-X-B method in LATE", Proc. 26th IAEA Fusion Energy Conference, Kyoto, Japan, 2016, IAEA-CN-234, EX/P4-45.
- [4] TANAKA, H. et al., "Electron Bernstein wave heating and current drive with multi-electron cyclotron resonances during non-inductive start-up on LATE", Proc. 27th IAEA Fusion Energy Conference, Ahmedabad, India, 2018, IAEA-CN-258, EX/P3-19.
- [5] MAEKAWA, T. et al., "Formation of spherical tokamak equilibria by ECH in the LATE device", Nucl. Fusion **45** (2005) 1439-1445.
- [6] YOSHINAGA, T., UCHIDA, M., TANAKA, H., MAEKAWA, T., "Spontaneous formation of closed-field torus equilibrium via current jump observed in an electron-cyclotron-heated plasma", Phys. Rev. Lett., **96** 125005 (2006).